Estimating Time Since Forest Harvest Using Segmented Landsat ETM+ Imagery

M. A. Wulder^[1], R. S. Skakun[2], W. A. Kurz[1], and J.C. White[1]

[1]Canadian Forest Service (Pacific Forestry Centre), Natural Resources Canada, Victoria, British Columbia.

[2]Canadian Forest Service (Northern Forestry Centre), Natural Resources Canada, Edmonton, Alberta.

^Corresponding Author

Michael Wulder
Canadian Forest Service, 506 West Burnside Road, Victoria, BC, V8Z 1M5
Email. mwulder@nrcan.gc.ca; Phone: 250-363-6090; Fax: 250-363-0775

Pre-print of published version.

Reference:
Wulder, M.A., R.S. Skakun, W.A. Kurz and J.C. White, 2004; Estimating Time Since Forest Disturbance Using Segmented Landsat ETM+ Imagery, Remote Sensing of Environment, 93, pp. 179-187.

DOI.
http://dx.doi.org/10.1016/j.rse.2004.07.009

Estimating Time Since Forest Harvest Using Segmented Landsat ETM+ Imagery

Abstract
Modeling of forest carbon (C) dynamics requires precise information regarding when a disturbance occurred and the age of regeneration present. Generally this information is obtained in the age class attribute of forest inventories, however forest inventories can become quickly outdated when disturbance events are not continuously integrated into the database. In this study, Landsat ETM+ image data and Tasseled Cap index values were used to estimate the age of lodgepole pine (*Pinus contorta*) stands from the approximate time of disturbance to 20 years of regeneration. An image segmentation procedure aided the removal of pixels representative of residual forest and other non-characteristic stand conditions within forest inventory polygons, in order to isolate the pixels representative of regenerating harvested forest. A stepwise multivariate regression procedure was used to estimate stand age for harvested areas, and an R^2 of 0.68 (with a standard error of less than 2.4 years) was computed. This transferable approach provides useful information for forest C accounting when the year of disturbance, or the age of subsequent regeneration is required for estimating C stocks.

Introduction
Forests play an important role in the global carbon (C) cycle. Forest C dynamics, particular in some boreal ecosystems, are strongly influenced by disturbance (i.e. fire, insect, harvest) and associated patterns of forest succession. A disturbed forest typically functions as a net C source through respiration and decomposition of dead organic matter. Forest regeneration following disturbance acts as a net C sink when the uptake of C in regenerating trees exceeds the initial loss of C. Modeling C dynamics in these forest conditions relies on precise information regarding when a disturbance occurred and the age of regeneration present. Trees or stands of trees killed by disturbance (i.e. fire, insect, harvest) generally act as a net carbon source, with C that had been sequestered as biomass being released. Forest regeneration following disturbance results in sequestration of C back into the ecosystem, where young and vigorously growing trees covert carbon dioxide (CO_2) from the atmosphere into biomass via photosynthesis (Karjalainen *et al*., 2000). As regenerating stands approach maturity, the size of the vegetation C pool may eventually equal or even surpass the pre-disturbance C stock levels (Dale *et al*., 1993). Because disturbance followed by regeneration represents only a temporary loss of C from the ecosystem, the period of time required for the formation of a new stand affects C dynamics.

Several investigators have shown a close relationship between the succession stage and spectral response of forests detected using Landsat Thematic Mapper (TM) data. Horler and Ahern (1986) found that TM bands 5 and 7 are particularly sensitive to forest vegetation density, especially in the early stages in the regeneration of a clear-cut. Foody *et al.* (1996) separated a range of tropical forest age classes (pasture, <2 years, 2-3 years, 3-6 years, 6-14 years, >14 years) with >85 % classification accuracy using TM bands 3, 4, and 5. Fiorella and Ripple (1993) found the “structural index” (TM bands 4/5) to have the highest correlation (R = 0.96) with stand age of young Douglas-firs (*Pseudotsuga*

menziesii (Mirb.) Franco). Kimes *et al*. (1996) used TM bands 3, 4, 5, elevation, slope, and aspect as inputs to a neural network classification for mapping conifer forests <50 years of age in western Oregon. In other studies, Cohen *et al*. (1995) found the TM-derived Tasseled Cap wetness index to be particularly useful for distinguishing various age classes (i.e., young, mature, and old-growth) of closed canopy conifer forest in the Pacific Northwest. Jakubauskas (1997) separated early lodgepole pine (*Pinus contorta* var. latifolia) succession stages in Yellowstone National Park, U.S.A. using texture information derived from TM data, Tasseled Cap index, and NDVI values. Helmer *et al*. (2000) examined successional montane tropical forest using multi-date TM-derived Tasseled Cap index values. Other investigators have utilized the NDVI (Sader *et al*., 1989), but concluded that the index was insignificantly correlated with regenerating forest age. Imagery with lower spatial resolution than Landsat has also been used to estimate the occurrence date of boreal forest fires. Fraser and Li (2002) present a method for estimating forest age (post-burn) using SPOT VEGETATION. Forest age was estimated with an RMS error of 7 years (r^2=0.7). Amiro and Chen (2002) built upon the methods of Fraser and Li (2002) in order to estimate fire scar ages by Canadian boreal ecoregion. While the ability to estimate the age of the fire scars decreased with time since fire, empirical regressions between scar age and a SPOT VEGETATION band ratio were found to be statistically significant for periods of 6 to 30 years, with RMS errors ranging from 5 to 12 years.

Forest inventories that store polygon data in a geographic information system (GIS) are a primary tool used by forest managers. The polygons are generalizations of forest characteristics typically derived from aerial photography. The polygons are delineated based on homogenous stand-structure characteristics, such as species composition, age, crown closure, and density class (Gillis and Leckie, 1993). The forest inventory information is often used to describe past disturbance regimes, as reflected in the age-class structure. The data from inventories may however lack the precision required for estimating C stocks of current forest conditions. Gillis and Leckie (1993) point out forest inventories in Canada are normally updated incrementally within approximately a ten-year cycle, suggesting the forest inventory information is often not all of the same vintage. A method to update forest inventory polygons to current forest conditions is desirable.

In this study, we examined the utility of remotely sensed data for estimating the stand age of regenerating forest. These estimated stand ages provide a useful information source for an operational forest C accounting framework (Kurz *et al*., 2002). Image values were extracted from a single-date Landsat ETM+ scene and used in conjunction with a GIS-based forest inventory to produce stand age estimates of regenerating lodgepole pine (*Pinus contorta*).

Study Area

The area selected for analysis is located in the Morice Forest District of British Columbia, Canada, and covers approximately 5,900 km^2 (82 km east/west by 72 km north/south), centered at latitude 54° 09’04.4 N and longitude 126° 33’32.1 W (Figure 1). The topography is rolling and gentle to the north and east and becomes mountainous in

the southwest. The climate is transitional between coast and interior, having a continental climate that is moderated by a coastal marine influence. The dominant tree species are lodgepole pine, white spruce (*Picea glauca* (Moench) Voss), and subapline fir (*Abies lasiocarpa* (Hook.) Nutt.). Other forest types include western red cedar (*Thuja plicata* Donn.), balsam fir *(Abies balsamea* (L.) Mill.), western hemlock (*Tsuga heterophylla* (Raf.) Sarg.), whitebark pine (*Pinus albicaulis* Engelm.), western larch (*Larix occidentalis* Nutt.), trembling aspen (*Populus tremuloides* Michx.), and balsam poplar (*Populus balsamifera* L.). The majority of harvesting activities are clear-cut and clear-cut with retention – a treatment that leaves a residual stand structure in the harvest cut to facilitate forest regeneration and provide shelter for wildlife. Most of this logging activity has occurred since 1980.

Data Collection, Preparation, and Analysis

Forest inventory polygons

For this study, GIS-based forest inventory polygons were used to extract forest stand age and species composition information. The majority of the inventory polygons within the study area were interpreted from aerial photography collected during a re-inventory of the study area in 1992. In each inventory polygon, stand age was assigned in years and species composition was delineated up to the fourth leading species with estimates of species percent to the nearest 10 percent. We stratified the inventory data set to obtain polygons <21 years of age, with lodgepole pine as the leading tree species. A total of 800 polygons out of a possible 1114 polygons, were retained from the stratification for analysis. The inventory and the subsequent data layers were projected to a UTM NAD 83 (Zone 10) projection.

Image processing

Landsat-7 ETM+ data were acquired September 15, 2001 over a cloud-free region of the Morice Forest District (path/row: 51/22). The image was obtained geometrically corrected (Wulder et al. 2002) and following close inspection of the image in conjunction with the forest inventory polygons, no additional geo-corrections were required. A Top-of-Atmosphere (TOA) reflectance correction based upon the theory of Markham and Barker (1986) was applied to ETM+ bands 1, 2, 3, 4, 5 and 7. The TOA procedure corrects for variations in solar illumination, atmospheric transmission and path radiance, and assumes a uniform atmosphere within the image (Peddle *et al*., 2003). The image is transformed from raw digital numbers to TOA reflectance values using image calibration values, radiometric ancillary information, solar zenith angle, and Earth-sun distance measurements. An at-satellite Tasseled Cap Transformation procedure was then applied to obtain brightness, greenness and wetness index values (Huang *et al*., 2002).

Data analysis and segmentation

The vector boundaries produced for forest inventories capture a homogeneous assemblage of forest attributes (Gillis and Leckie, 1993). As a result, when observing individual pixels within a polygon, the variability between values can be high (Wulder, 1998). Wulder *et al*. (1999) illustrated the disagreement between forest inventory attribute information and remotely sensed spectral values found within polygons. To account for the variability in spectral properties within forest inventory polygons, we

used a segmentation procedure to group neighboring pixels according to the similarity of their spectral properties. Polygon decomposition (Wulder and Franklin, 2001) is an approach that enables the high within-polygon variability of pixel values to be utilized by providing a context for analysis and comparison. Further, within each forest inventory polygon, the segmentation procedure results in the stratification of the pixels into polygonal sub-units, based on local homogeneity of the pixel values present. A rule-base can then be applied to select and use in the estimation of age, only those pixel values that represent post-harvest conditions and exclude any residual stand structure not indicative of post-harvest conditions. For comparison, age estimates are also made from within polygon pixel values that are not subject to a segmentation and vetting process.

Precedents in the literature indicated the utility of empirical modeling, or regression based approaches to estimate stand age. Independent variables utilized include Landsat bands 3, 4, 5, and 7, and the Tasseled Cap components of brightness, greenness, and wetness. In turn, regression equations are developed using the age attribute in the forest inventory as the dependant variable. ETM+ reflectance and Tasseled Cap components were extracted from each forest inventory polygon and polygon segment and imported into Stata version 7.0 (Stata Corporation, 2001) for analysis. Descriptive statistics were calculated to verify that ETM+ reflectance and Tasseled Cap index values varied with changes in age. The mean values within each of the forest inventory polygons and polygon segments were then calculated for each of the above mentioned independent variables and used in the analysis. The correlation analysis was conducted to determine which ETM+ bands and Tasseled Cap indices were significantly related to stand age.

Univariate regression models were generated to determine how well ETM+ spectral response and Tasseled Cap components could estimate stand age. Multivariate regression was then applied using a stepwise-variable selection procedure to determine which of those variables used in the univariate regression should be accounted for in the model. The stepwise procedure initially enters into the model the variable that has the highest correlation with stand age. At each subsequent step, the variable with the next highest correlation is added. Each variable was tested for removal based on statistical significance ($\alpha = 0.95$). The final regression model was built after it was determined that no more variables could be entered or removed. Model strength was assessed by the R^2 value and root mean square error. Models exhibiting multicollinearity were discarded.

Age estimates were made from mean reflectance values and Tasseled Cap components found, 1) within forest inventory polygons, and; 2) within spectrally similar within-polygon segments. In the first procedure, estimates of stand age were based on the mean value of all image pixels contained in a forest inventory polygon, including residual forest and forestry road networks. In the second procedure, the image pixels representing these features and other non-characteristic stand conditions were removed and the mean value of the remaining image pixels in a polygon segment were used to estimate stand age. A segment-based area weighted average is used to generate an age estimate from within polygon segments to represent the age of a given polygon. The segments were created using eCognition version 2.1 (Definiens Imaging, 2002). The proprietary algorithm essentially minimizes the average heterogeneity of the image by segmenting

features based upon similarities in shape, colour, size and texture. User settings control the nature of the segmentation. For instance, if the scale parameter is larger, the image objects will be larger. In this case, the following settings were used for scale (10), colour (0.6), shape (0.4), smoothness (0.5), and compactness (0.5).

The main operations to remove the non-characteristic stand conditions were:

1. Buffer 30 meters inward from the perimeter of the forest inventory polygon to reduce possible edge effects (Boudewyn *et al.*, 2000);
2. Segment the forest inventory polygons into contiguous, homogeneous image units (with parameters described above);
3. Removed polygon segments that were uncharacteristic of a harvest clear-cut. For example, we determined that polygon segments with a shape index >2.4 are relatively linear in shape (i.e. forest access roads and cut block edges) and should be removed. We also removed polygon segments <1 ha in size, as harvest clear-cuts are generally larger and these small units are also highly influenced by edge conditions.
4. Created a rule-base that retains polygon segments that have spectral characteristics that are closest to TM channel 4 mean values found within a given forest inventory polygon and that compose at least one third of that same polygon's area. The rule implies that polygon segments such as residual forest, secondary successional species or rocky outcrops would have mean values further from the mean value of the forest inventory polygon, which are not representative of the post-harvest areas regenerating within a stand.

A total of 1305 polygon segments were created, which is approximately 65% more discrete units than were contained in the original forest inventory (with 800 polygons) (Table 1). The mean area of the generated segments was 9.2 ha, a decrease from the 27.0 ha mean of the forest inventory polygons.

Results

Polygon Segment Illustrations

Four forest inventory polygons were selected for illustration of the polygon segmentation procedure (Figure 2). The wider vectors that encircle the entire harvest cut area indicate the original forest inventory polygon. The thinner vectors represent the polygon segments within the inventory polygon, derived from the segmentation procedure. An "x" indicates a segment that has a mean value closest to the forest inventory mean and composes at least one third of the polygon area, and would have been used for estimating stand age. The ages of Polygons A, B, C and D are 5, 6, 7, and 13 years respectively.

In Figure 2 polygons A, B and C show examples of harvest operations in which residual forest remains inside the harvested area. The residual forest has a different reflectance pattern than the regenerating forest. The regenerating forest is bright and pink, indicating high reflectance from early successional trees and shrubs, whereas the residual forest has a darker green tone indicative of a closed canopy structure. The polygon segmentation procedure uses information related to shape, color, size and texture to create locally homogenous objects. Using the rule-base, the segments representing regenerating forest

are kept (marked on the figure with an “x”) and residual forest and other non-representative stand conditions are removed. In Polygons A and B, the lower segments with an “x” were marked first and the upper segments next, which indicates the lower segments had a TM channel 4 mean value closer to the mean of the forest inventory polygon and the upper segments had the next closest TM channel 4 mean value and were included, as they composed at least one third of the inventory polygon area. Polygon D is an example of an older harvest cut where a small patch in the stand has limited vegetation growth. These characteristics may be due factors such as poor soil conditions, a rocky outcrop, or from soil compaction of heavy machinery during harvest operations. In this example, a large polygon segment with a homogeneous green tone is marked with an “x”. The other large segment above, although similar in size and color, was not marked with an “x” because the mean value did not meet the required criteria (as the desired one-third of the polygon was already accounted for). A smaller patch of vegetation growth was also segmented yet was removed from the empirical analyses (as were all segments with an area <1 ha).

Stand wetness characteristics

Table 1 shows the mean wetness values and mean standard deviations of forest inventory polygons and polygon segments over the 4-20 year age distribution (no polygons of ages 1, 2, or 3 existed in the inventory). Generally, wetness increased from the approximate time of disturbance to a regeneration of 20 years (Figure 3a). The mean wetness of polygon segments in early stages of succession (<10 years) is also slightly less than the mean wetness of inventory polygons. This likely results from removing residual forest pixels from the polygon, since the wetness signature would be less influenced by small patches of forest and more by the reflectance properties of regenerating trees. In Figure 3b, the large reduction in mean standard deviation for polygon segments supports how polygon segmentation reduces in-polygon variability. Stands 4 years of age had a very low standard deviation, indicating a homogeneity of stand structural conditions, which is also illustrated by no within-polygon segments being generated (Table 1). Additionally, polygons of 4 years have only three forest inventory polygons available for analysis.

Correlation coefficients between stand age and digital numbers

In general, stand age was negatively correlated with Landsat ETM+ spectral response (Table 2). Similar relationships have been identified in tropical (Mausel *et al*., 1993) and temperate (Jakubauskas, 1996) forest regions. The strongest correlations for both forest inventory polygons and polygon segments were ETM+ bands 3 (visible), 5 (mid-infrared) and 7 (mid-infrared), with *R*- values of –0.78, -0.78 and –0.77, respectively, for segments. Reductions in band 3 reflection are generally caused by increases in chlorophyll absorption as leaf area and biomass increase with stand age. Decreases in middle-infrared reflectance (ETM+ bands 5 and 7) may have been the result of increased water absorption and canopy shadowing. Similarly, a weak negative correlation in band 4 (near-infrared), with an *R*-value of –0.19, may have also been influenced by increased shadowing resulting from canopy structure. Overall, the correlation coefficients between stand age and image values were higher for polygon segments than for the original inventory polygons.

The strongest correlation to stand age using Tasseled Cap index values was the wetness index, with *R*-values of 0.56 for the forest inventory polygons and 0.78 for polygon segments (Table 2). Landsat TM wetness has been shown in previous studies to be highly correlated with stand age of mature forest structures (Cohen and Spies, 1992; Hansen *et al*., 2001), but only few studies have used wetness in the context of forest succession (Jakubauskas, 1997; Helmer *et al*., 2000). The brightness index, a positive linear combination of all six bands, had the next highest correlations; R = -0.39 for inventory polygons and –0.61 for polygon segments. Negative brightness correlations may have been caused by reduced ground exposure due to increased crown closure with canopy development. Positive greenness correlations, R = 0.27 for inventory polygons and 0.44 for polygon segments, may have been related to increased amounts of green vegetation in the pixel. Again, all correlation coefficients were higher for polygon segments in comparison to the original inventory polygons.

Estimates of stand age using univariate and multivariate regression

Univariate and multivariate regression estimates to stand age were the strongest when image values from polygon segments were used (Table 3b) as opposed to the polygons (Table 3a). Landsat ETM+ bands 3, 5, 7 and the wetness index all generated the highest R^2 values in a univariate regression model; the root mean square error was <2.5 years for each independent variable. The results for band 4 univariate models were the least significant. For the multivariate stepwise regression procedure (with independent variables of ETM+ bands 3, 5, 7, and wetness), the polygon segments produced an R^2 value of 0.68 and <2.4 years of error, which is the highest of all estimates to stand age in this study.

Figure 4 is a plot of the residual values generated from the multivariate regression using the polygon segments. The regression line is also shown expressing the prediction of age given the multiple variables. As stand age increases, the variability of the residual values from the regression line increases. This indicates that the strength of the regression model becomes weaker with increases in stand age. Since the younger stands had the least amount of deviation from the regression line, the image values from these stands would have generated the strongest influence on model strength. To verify this, we applied a multivariate regression to stand ages of 4 to 10 years only and generated an R^2 value of 0.71 (with a standard error of 2.18). This younger age range is generally within normal forest inventory update cycles and of prime interest to C modeling.

Discussion

In this study, we reduced within-polygon variability by removing pixels representing residual forest and other non-representative stand conditions from within pre-defined forest inventory polygons. From a C accounting perspective, these features still contribute to the net C balance of the harvested area and would provide useful information in a forest inventory database. For example, data on the size and age of the residual forest in a forest inventory could be used in C models for computing changes in C stocks post-harvest. However, estimating inventory attributes of the polygon segments that represent residual forest would be problematic. In Figure 2, we can see Polygons A, B and C have some segments composed of both regenerating forest and residual forest;

no segments in these examples are “pure” residual forest. As a result, these mixed segments of residual and regenerating forest would have high within-segment variation, poor relationships with stand age, and could perhaps only be inventoried with categorical descriptors, such as “high vegetated” and “low vegetated”. Other segments with non-representative stand conditions such as forestry access roads and rocky outcrops, which are not shown in these examples, lower the net C balance. An inventory of these features would also be useful in a forest inventory database, but similar difficulty would likely exist by the within-segment variability.

The objective of this study was to estimate the ages of regenerating forest using remotely sensed data. We observed the direction and strength of the relationship between stand age and ETM+ bands 3, 4, 5 and 7 and brightness, greenness, and wetness indices. Band 3 developed a strong relationship with stand age in a negative direction; this is due to a decrease in reflectance from an increase in chlorophyll absorption. Band 4 and the greenness index generated poor relationships with stand age - likely due to variability in broad-leaf vegetation caused by successional shrubs and herbs. Bands 5 and 7 and the brightness index had strong and negative relationships which were thought to have been caused by increased shadows due to variable heights from the developing stand structure. The wetness index showed a strong and positive relationship to stand age, indicating healthy forest growth. The wetness index could also be valuable in providing information on stands that have poor regeneration.

The results of this analysis are inline with those of other studies using similar approaches; Kimes *et al*. (1996) achieved a maximum R^2 value of 0.69 with approximately 5.50 years of error using TM bands 3, 4, 5, elevation, slope, and aspect data for conifer forest stands <50 years of age. Fiorella and Ripple (1993) generated an R^2 of 0.54 for conifer stands <18 years of age using TM band 4, however their model was built using only a sample of 45 regenerated stands. Overall, bands 3, 5, 7 and the Tasseled Cap wetness index were the most successful independent variables for estimating stand age and were the variables used in a multivariate regression model. The coefficients generated from this model, however, are empirical in nature and limited to the area of study and the species of interest. While the actual coefficients used are specific to this study, the approach is transferable to other locations and/or species of interest. Furthermore, although this approach only focused on disturbances caused by harvest, the approach could be extended to other forms of disturbance.

Conclusion

In this study, we used Landsat ETM+ image data and Tasseled Cap index values in conjunction with a GIS-based forest inventory polygon dataset to determine how well remotely sensed data could be used to estimate the ages of regenerating forest. The context is placed in a C accounting framework; if the date of disturbance is known, then C models can be adjusted to compensate for initial C losses followed by C sequestration in regenerating trees. The period of regeneration from which stand age was estimated were ages 4 to 20 years.

Estimates of stand age were obtained for both forest inventory polygons and within-polygon units. For the latter, a procedure was used to segment the forest inventory polygons into smaller polygonal sub-units, and a rule-base was developed that removed all sub-units uncharacteristic of the stand's age. For example, the rule-base enabled removal of residual forest and access roads from the polygon interior. The use of the polygon segments was more successful for generating an estimate of stand age as indicated by the larger correlation coefficient values and the univariate and multivariate regression models. The highest coefficient correlation to stand age was an *R*-value of 0.78, based on the wetness index. A stepwise multivariate regression procedure generated a regression value of $R^2 = 0.68$, with a standard error of 2.39 years. Further, it was demonstrated that these results might be improved when constraining the date range of the training data to younger ages only (in this case, <10 years). From a C modeling perspective, the ability to estimate stand age to within 3 years, where no other current age information is available, provides a useful optional model input.

Acknowledgements

The authors would like to thank David Seemann of the Canadian Forest Service for assisting with the data analysis. Steen Magnussen of the Canadian Forest Service is also thanked for valuable discussions during the project planning stages. The Top-of-Atmosphere calibration and correction routine used in this research was generously provided by Robert Landry, of the Canada Centre for Remote Sensing. Government of Canada funding support, from the Climate Change Action Fund (http://www.climatechange.gc.ca), is gratefully noted.

References

Amiro, B., and J. Chen. 2003. Forest-fire-scar aging using SPOT VEGETATION for Canadian ecoregions. *Canadian Journal of Forest Research*, 33: 1116-1125.

Boudewyn, P., Seemann, D., Wulder, M. and Magnussen, S. 2000. The effects of polygon boundary pixels on image classification accuracy. In *Proceedings of the 22nd Symposium of the Canadian Remote Sensing Society, Victoria, British Columbia, August 20th to 25th, 2000. Remote sensing and spatial data integration: measuring, monitoring and modeling.*

Cohen, W.B. and T.A. Spies. 1992. Estimating structural attributes of Douglas-fir/Western Hemlock forest stands from Landsat and SPOT imagery. *Remote Sensing of Environment*, 41: 1-17.

Cohen, W.B., T.A. Spies, and M. Fiorella. 1995. Estimating the age and structure of forests in a multi-ownership landscape of western Oregon, U.S.A. *International Journal of Remote Sensing*, 16(4): 721-746.

Dale, V.H, R.V. O'Neill, M. Pedlowski, and F. Southworth. 1993. Causes and effects of land-use change in central Rondonia, Brazil. *Photogrammetric Engineering and Remote Sensing*, 59(6): 997-1005.

Definiens Imaging. 2002. eCognition Software: Release 2.1. Munich, Germany.

Fiorella, M. and Ripple, W.J. 1993. Analysis of conifer forest regeneration using Landsat Thematic Mapper data. *Photogrammetric Engineering and Remote Sensing*, 59(9): 1382-1288.

Foody, G.M., G. Palubinskas, R.M. Lucas, P.J. Curran, and M. Honzak. 1996. Identifying terrestrial carbon sinks: classification of successional stages in regenerating tropical forest from Landsat TM data. *Remote Sensing of Environment*, 55: 205-216.

Fraser, R.H., and Z. Li. 2002. Estimating fire-related parameters in boreal forest using SPOT VEGETATION, *Remote Sensing of Environment*, 82: 95-110.

Gillis, M., and D. Leckie. 1993. Forest inventory mapping procedures across Canada. Forestry Canada, PNFI, Information Report PI-X-114, 79p.

Hansen, M.J., S.E. Franklin, C. Woudsma, and M. Peterson. 2001. Forest structure classification in the North Columbia mountains using the Landsat TM Tasseled Cap wetness component. *Canadian Journal of Remote Sensing*, 27(1): 20-32.

Helmer, E.H., S. Brown, and W.B. Cohen. 2000. Mapping montane tropical successional stage and land use with multi-date Landsat imagery. *International Journal of Remote Sensing*, 21(11): 2163-2183.

Horler, D.N.H. and F.J. Ahern. 1986. Forestry information content of Thematic Mapper data. *International Journal of Remote Sensing*, 7: 405-428.

Huang, C., Wylie, B., Homer, C., Yang, L., and Zylstra, G. 2002. Derivation of a Tasseled cap transformation based on Landsat 7 at-satellite reflectance: *International Journal of Remote Sensing*, 23(8): 1741-1748.

Jakubauskas, M.E. 1996. Thematic Mapper characterization of lodgepole pine seral stages in Yellowstone National Park, USA. *Remote Sensing of Environment*, 56: 118-132.

Jakubauskas, M.E. 1997. Effects of forest succession on texture in Landsat Thematic Mapper imagery. *Canadian Journal of Remote Sensing*, 23(3): 257-263.

Karjalainen, T., G J. Nabuurs, J. Liski, A. Pussinen, T. Lapvetelainen, and T. Eggers. 2000. Ten most frequently asked questions: carbon sequestration in forests. EFI News, pp. 5-7.

Kimes, D.S., B.N. Holben, J.E. Nickeson, and W.A. McKee. 1996. Extracting forest age in a Pacific Northwest forest from Thematic Mapper and topographic data. *Remote Sensing of Environment*, 56: 133-140.

Kurz, W.A., M. Apps, E. Banfield, and G. Stinson. 2002. Forest carbon accounting at the operational scale. *The Forestry Chronicle*, 78(5): 672-679.

Markham, B. and J. Barker. 1986. Landsat MSS and TM post calibration dynamic ranges, exoatmospheric reflectances and at satellite temperature. EOSAT Landsat Technical Notes, 1: 3-7.

Mausel, P., Wu, Y., Li, Y., Moran, E.F., and Brondizio, E.S. 1993. Spectral identification of successional stages following deforestation in the Amazon. Geocarto International, 8(4): 61-71.

Peddle, D., P. Teillet and M. Wulder. (2003). Radiometric image processing, In pp. 181-208, M. Wulder and S. Franklin, (Editors). *Remote Sensing of Forest Environments: Concepts and Case Studies*, (Kluwer Academic Publishers, Boston).

Sader, S.A., R.B. Waide, W.T. Lawrence, and A.T. Joyce. 1989. Tropical forest biomass and successional age class relationships to a vegetation index derived from Landsat TM data. *Remote Sensing of Environment*, 28: 143-156.

Stata Corporation. 2001. Stata Statistical Software: Release 7.0. College Station, TX.

Wulder, M. 1998. Forest polygon decomposition through the integration of remote sensing, GIS, UNIX, and C. *Computers & Geosciences*, 24(2): 151-157.

Wulder, M., S. Magnussen, P. Boudewyn, and D. Seemann. 1999. Spectral variability related to forest inventory polygons stored within a GIS. Presented at the IUFRO Conference on Remote Sensing and Forest Monitoring, Rogow, Poland, June 1 to 3, 1999.

Wulder, M. and S. Franklin. 2001. Polygon decomposition with remotely sensed data: Rationale, methods, and applications. *Geomatica*, 55(1): 11-21.

Wulder, M., E. Loubier, and D. Richardson, 2002. A Landsat-7 ETM+ orthoimage coverage of Canada. Canadian Journal of Remote Sensing. 28(5): 667-671.

List of Figures and Tables

List of Figures

List of Tables

Table 1.

		Forest Inventory Polygons				Polygon Segments			
		Count (#)	Area (ha)˜	Wetness (DN)		Count (#)	Area (ha)	Wetness (DN)	
				mean	std dev			mean	std dev
Stand Age	4	3	5.79	-73.4	4.5	3	5.79	-73.4	4.5
	5	26	14.6	-63.8	18.2	34	7.8	-67.3	13.8
	6	45	20.4	-56.9	15.3	75	9.4	-60.3	11.1
	7	9	39.5	-49.9	12.2	16	14.5	-56.9	9.3
	8	17	19.1	-52.2	14.7	25	9.6	-55.6	8.6
	9	24	16.2	-42.2	17.1	37	7.9	-49.9	11.2
	10	43	17.1	-38.5	12.4	64	7.1	-40.5	9.8
	11	102	21.2	-34.9	12.2	165	7.8	-36.2	10.2
	12	93	26.7	-31.4	11.9	157	9.2	-30.0	11.1
	13	89	48.2	-25.7	12.3	149	10.6	-26.4	10.3
	14	63	30.6	-25.4	11.1	103	8.3	-23.8	9.8
	15	63	29.1	-23.9	10.1	105	7.5	-22.8	9.4
	16	63	38.7	-21.8	10.0	102	8.9	-20.4	8.1
	17	45	28.7	-20.5	9.1	72	10.7	-19.7	8.4
	18	62	38.0	-17.6	8.3	104	10.0	-16.8	7.5
	19	25	28.0	-14.4	7.3	41	10.7	-14.4	6.1
	20	28	36.3	-14.2	7.1	53	10.9	-14.1	5.5
General Polygon Description:									
Total Count		800				1305			
Average Area		27.0				9.2			

˜Note: Area (ha) estimates represent mean polygon size.

Table 2.

	Forest Inventory Polygons	Polygon Segments
	R	*R*
ETM+ 3	-0.53	-0.78
ETM+ 4	-0.18	-0.19
ETM+ 5	-0.56	-0.78
ETM+ 7	-0.54	-0.77
Brightness	-0.39	-0.61
Greenness	0.27	0.44
Wetness	0.56	0.78

Note: All correlations significant at 95% ($p = 0.05$).

Table 3a.

Univariate Regression			
	Regression Equation	R^2	Root Mean Square Error
ETM+ 3	-0.342x + 21.19	0.28	2.96
ETM+ 4	-0.020x + 15.63	0.01	3.48
ETM+ 5	-0.106x + 19.26	0.31	2.90
ETM+ 7	-0.178x + 17.83	0.29	2.94
Brightness	-0.085x + 23.46	0.15	3.22
Greenness	0.082x + 11.45	0.07	3.37
Wetness	0.110x + 16.89	0.31	2.90
Stepwise Multivariate Regression			
Regression Equation: -0.137wetness – 0.116etm7 + 0.059greenness + 16.24			
R^2: 0.46			
Root Mean Square Error: 2.83			

Note: All regressions significant at 95% ($p = 0.05$).

Table 3b.

Univariate Regression			
	Regression Equation	R^2	Root Mean Square Error
ETM+ 3	-0.625x + 27.09	0.60	2.43
ETM+ 4	-0.044x + 17.54	0.02	3.82
ETM+ 5	-0.177x + 22.73	0.61	2.41
ETM+ 7	-0.307x + 20.54	0.60	2.44
Brightness	-0.177x + 33.63	0.37	3.06
Greenness	0.175x + 8.48	0.19	3.48
Wetness	0.181x + 18.71	0.61	2.42
Stepwise Multivariate Regression			
Regression Equation: 0.456wetness + 0.410etm7 – 0.387etm3 + 0.142etm5 + 18.20			
R^2: 0.68			
Root Mean Square Error: 2.39			

Note: All regressions significant at 95% ($p = 0.05$).

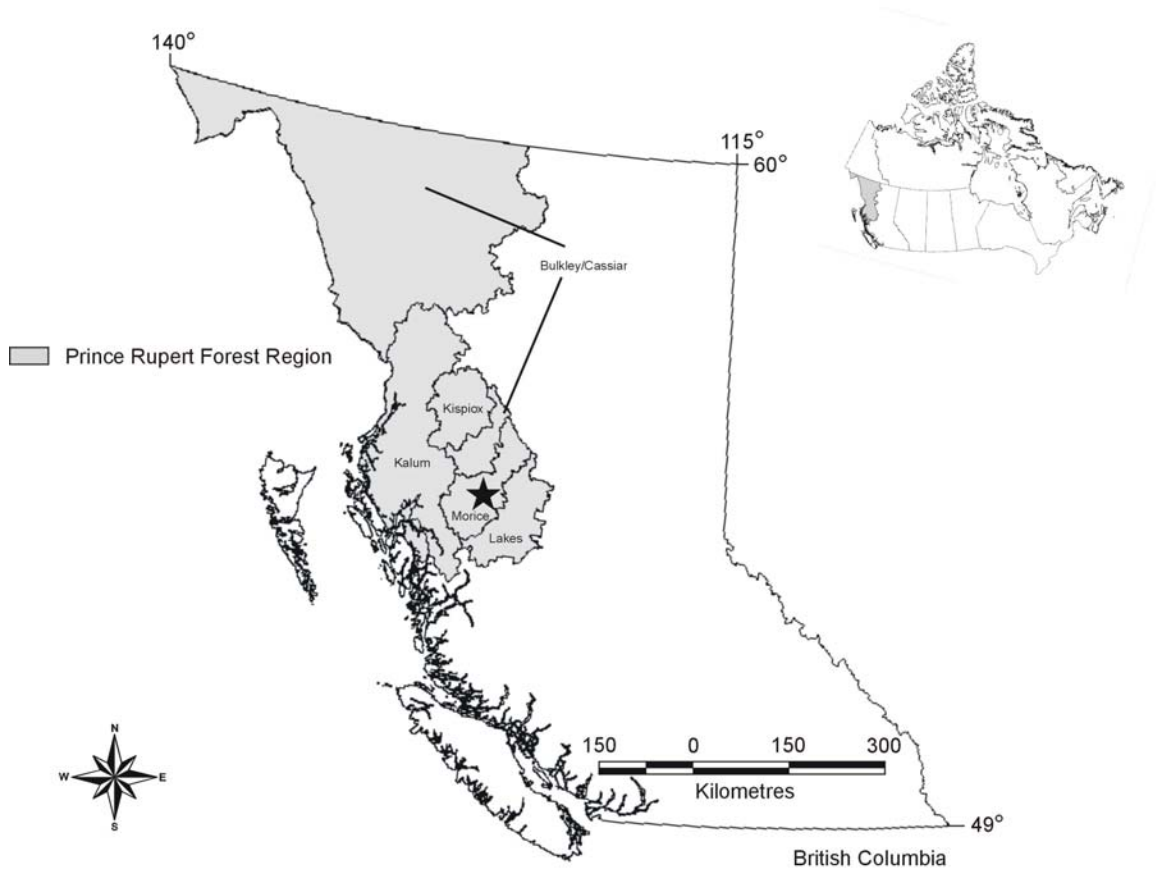

Figure 1. Study area located in the Morice Forest District, British Columbia, Canada.

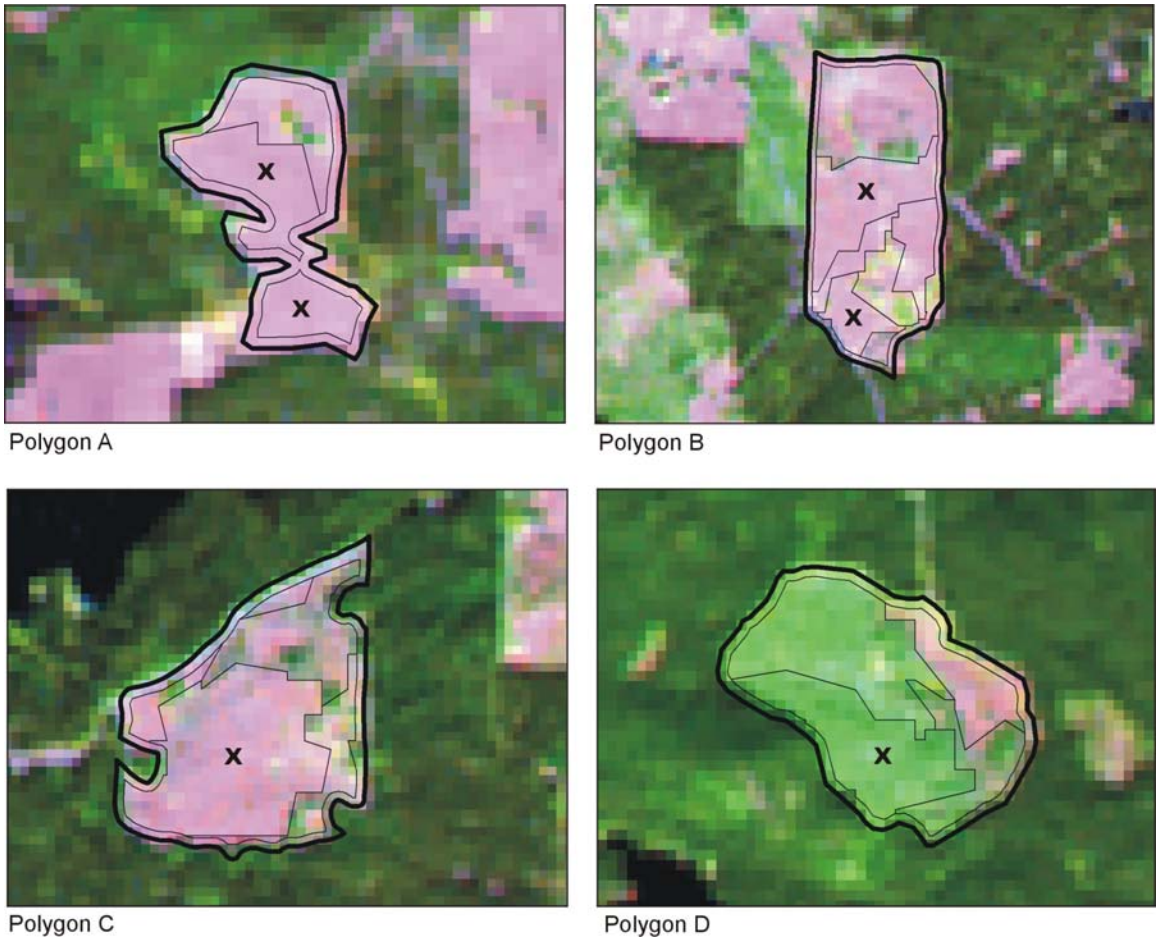

Figure 2. Illustrative examples of polygon segmentation for four forest inventory polygons (Polygon A, B, C, and D). A Landsat ETM+ image is shown in the background using RGB 543.

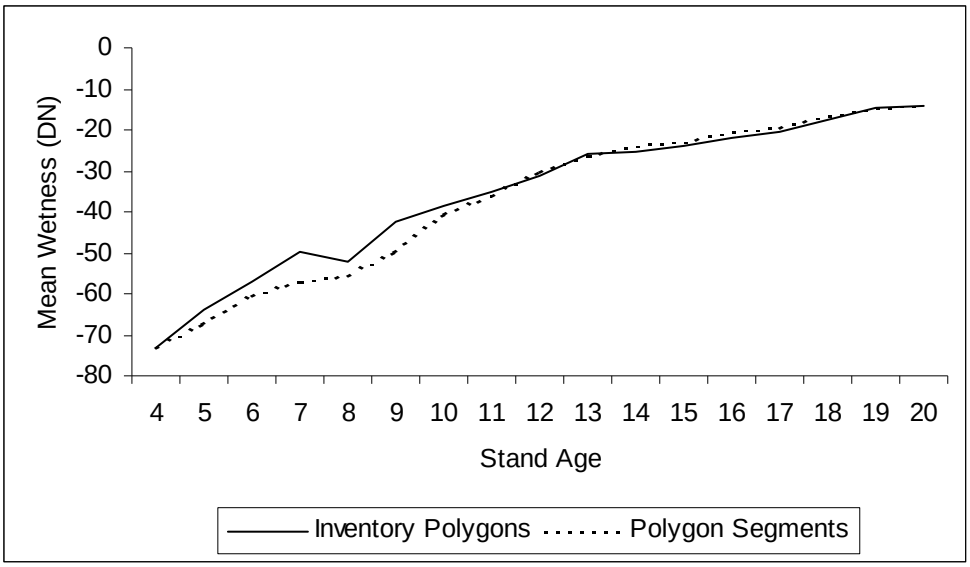

Figure 3a. Mean wetness values for regenerating forest stands aged 4 to 20 years.

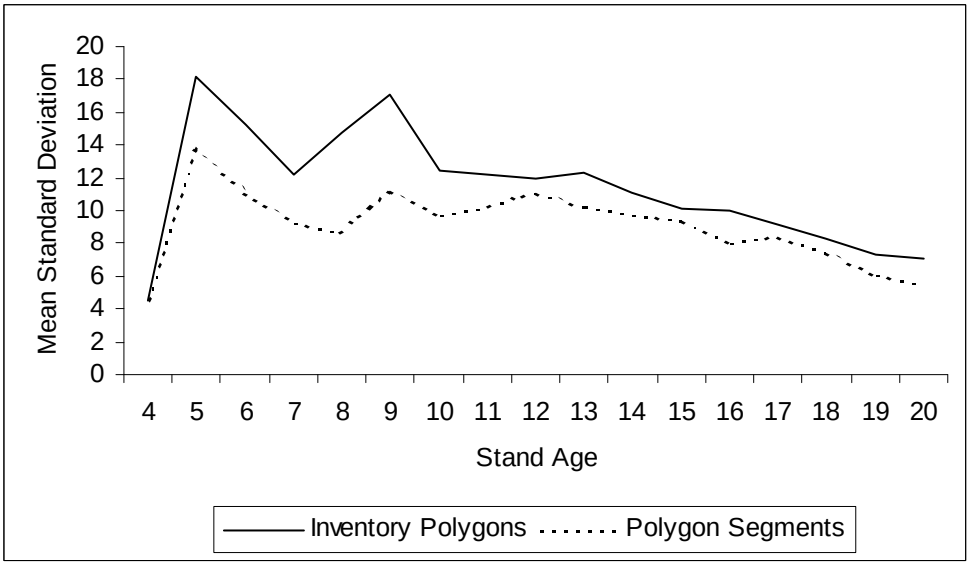

Figure 3b. Mean standard deviations for regenerating forest stands aged 4 to 20 years.

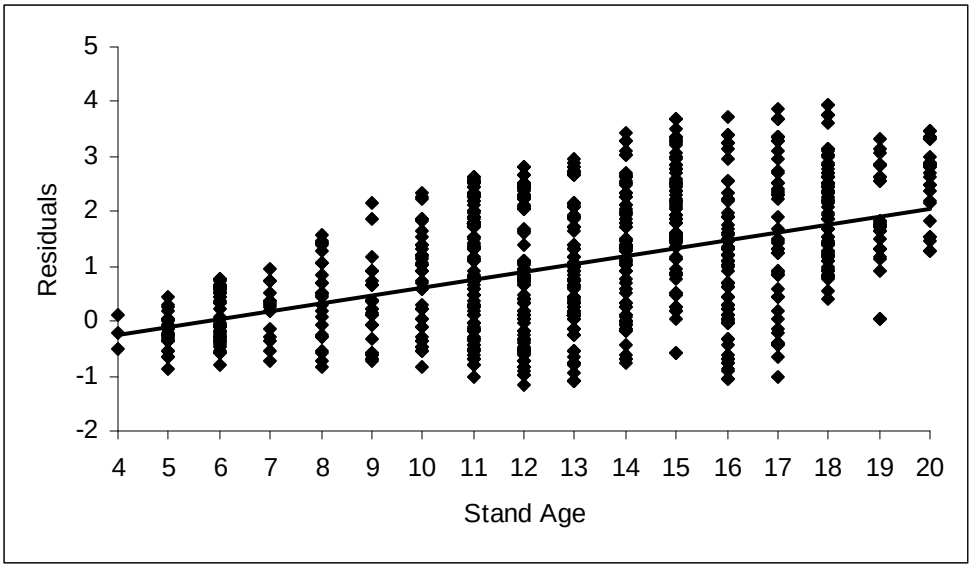

Figure 4. Residual values and regression fit generated from the multivariate regression procedure using the polygon segments.